



Cite this: *Chem. Commun.*, 2022, **58**, 7968

Received 27th May 2022,
Accepted 18th June 2022

DOI: 10.1039/d2cc03010a
rsc.li/chemcomm

Janus faced fluorocyclohexanes for supramolecular assembly: synthesis and solid state structures of equatorial mono-, di- and trialkylated cyclohexanes and with tri-axial C–F bonds to impart polarity†

Thomas J. Poskin,^a Bruno A. Piscelli,^b Keigo Yoshida,^c David B. Cordes,^a Alexandra M. Z. Slawin,^a Rodrigo A. Cormanich,^b Shigeyuki Yamada,^c and David O'Hagan ^a ^{*a}

Concise and general synthesis protocols are reported to generate all-*syn* mono-, di- and tri-alkylated cyclohexanes where a single fluorine is located on the remaining carbons of the ring. The alkyl groups are positioned to lie equatorially and to have triaxial C–F bonds imparting polarity to these ring systems. Intermolecular electrostatic interactions in the solid-state structure of the trialkylated systems are explored and the resultant supramolecular order opens up prospects for design in soft materials.

We have demonstrated that certain arrangements in selectively fluorinated cyclohexanes possess highly polar properties, particularly if the fluorines are strategically located on one face of the cyclohexane ring.¹ All-*syn*-1,2,3,4,5,6-hexafluorocyclohexane **1** is the flagship molecule in this regard, and its unusual polarity is evinced by a very high melting point (mp \sim 208 °C) as well as a high molecular dipole of μ = 5.89 D.² The origin of this polarity lies predominantly in the tri-axial alignment of three of the six C–F bonds, a situation that is always maintained in interconverting chair conformations. This imparts a polarity to the molecule and generates an electronegative (fluorine) and electropositive (hydrogen) face and the rings tends to associate electrostatically (hydrogen to fluorine faces) in the solid-state, with fluorine to hydrogen contacts, rather than fluorous clustering.^{3,4} The term 'Janus faced' cyclohexane⁵ has been applied to such cycloalkanes for this reason.

Given that the alignment of the axial C–F bonds is particularly significant in terms of inducing polarity in these systems, it can be anticipated that if the equatorial C–F bonds are replaced with alkyl groups, the polarity should be maintained. This was exemplified recently in the solid-state structures of a range of monoalkylated pentafluorocyclohexyl derivatives, where it emerged that the rings adopt the most polar conformation with triaxial C–F bonds and an equatorial alkyl substituent.⁶ Theory offers partial support where the methyl substituent in, for example, cyclohexane **2** illustrated in Fig. 1, has a small energy preference (-0.51 kcal mol⁻¹) for the equatorial methyl conformation.^{6a} In this paper we demonstrate an increasing

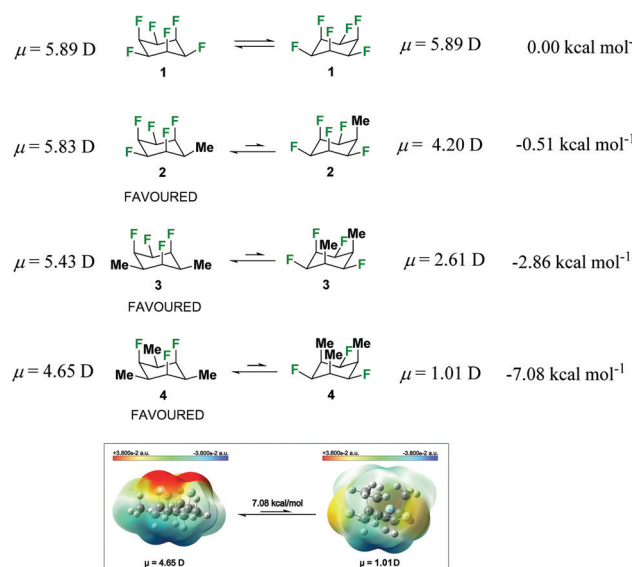


Fig. 1 Structures of **1–4** optimized at the B3LYPD3/def2-TZVP theory level, with calculated conformational Gibbs free energy differences and molecular dipole moments between the chair conformations of some selectively fluorinated all-*syn* fluorocyclohexanes.⁷ The lower image shows a surface electrostatic potential map for the conformers of **4**.

^a University of St Andrews, School of Chemistry, North Haugh, St Andrews, Fife, KY16 9ST, UK. E-mail: d01@st-andrews.ac.uk; Fax: 01334 463800; Tel: 01334 467171

^b University of Campinas, Chemistry Institute, Monteiro Lobato Street, Campinas, São Paulo, Brazil 13083-862. E-mail: cormanich@unicamp.br

^c Faculty of Molecular Chemistry and Engineering, Kyoto Institute of Technology, Matsusasaki, Sakyo-ku, Kyoto, 606-8585, Japan

† Electronic supplementary information (ESI) available. CCDC 2174305–2174309. For ESI and crystallographic data in CIF or other electronic format see DOI: <https://doi.org/10.1039/d2cc03010a>



preference for the triaxial C–F conformer with di- and tri-alkylated derivatives. This is predicted by the computational outcomes presented in Fig. 1 for cyclohexanes **3** and **4**. Progressive methylation at alternate positions around the ring is predicted to increase the triaxial C–F preference and increase the bias towards the more polar arrangements. The calculated⁷ molecular dipole moments (μ) for the conformers of **4** indicate that it is the triaxial arrangement of the fluorines which contributes most significantly to molecular polarity ($\mu = 4.65$ D), the ring inverted conformer with equatorial fluorines is much less polar ($\mu = 1.01$ D). With this background it became an objective to prepare a range of all-*syn* 2,4,6-trialkylated-1,3,5-trifluorocyclohexanes **16**, to assess their structures and properties, particularly as they are predicted to be strongly trifluoro-triaxial with the more polar conformations dominating. A general route was devised to this class of compounds which also allowed mono- and di-alkylated cyclohexane rings of this class to be prepared as shown in Scheme 1.

The syntheses sequences start with Sonogashira protocols⁸ coupling the appropriate commercially available fluorooiodobenzene **5**, **9** or **13** with terminal acetylenes. The resultant aryl-acetylenes **6**, **10a–c** or **14a–f** were then hydrogenated under standard conditions over Pd/C to generate alkyl-fluoroaryls **7**, **11a–c** or **15a–f** respectively with saturated side chains. These products were then subject to aryl ring hydrogenations under the conditions recently reported by Glorius⁸ for the preparation of fluorocyclohexanes from aromatic precursors, using the [CAAC]-COD Rh catalyst **17**.⁹ Although these aryl hydrogenation reactions proved to be slow (H_2 , 50–70 bar, 1–10 d) conversions overall are moderate to good and it offered a direct approach to this class of compounds generating products **8**, **12a–b** and **16a–f** as illustrated in Fig. 2. Some of the products were amenable to X-ray structure analysis, such as the monosubstituted derivative **8**, the disubstituted derivative **12c** and trisubstituted trifluorocyclohexanes **16d**, **16e** and **16f**. The offset in the stacking arrangement of the fluorocyclohexyl rings, as observed for the

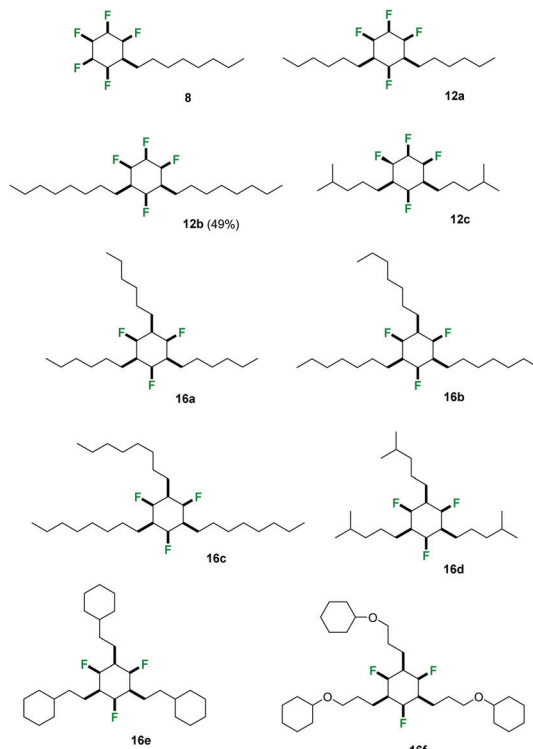
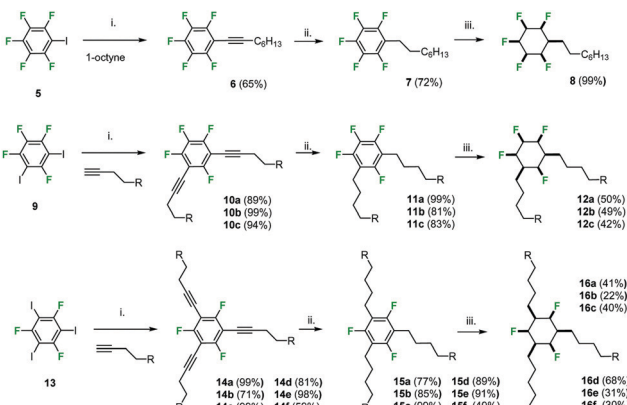


Fig. 2 Structures of the product mono-**8**, di-**12a–b** and tri-**16a–f** fluoroalkylated cyclohexanes prepared in this study.

monosubstituted derivatives^{2,6} was not observed for the di- and tri-substituted systems.

On the other hand, in the cases of the di- and tri-substituted derivatives **12c**, **16d** and **16e**, the cyclohexane rings stack directly, one on top of another as illustrated in Fig. 3 for **16e** (see also Fig. SI6–SI8, ESI†). It is also interesting to note that the alkyl substituents in the di- and tri-substituted systems lie in the plane of the stacked rings very different to the monosubstituted all-*syn* pentafluorocyclohexyl systems such as **8** and as previously disclosed in other cases where there is an angular herringbone arrangement of the side chains to the rings in the solid-state.^{6a} The more ordered stacking arrangement of the trialkyls **16** as a class was explored computationally in the dimeric and trimeric molecular assemblies for compound **4** as a model.

The surface electrostatic potential map for the triaxial arrangement of the fluorines in **4** as illustrated in Fig. 1,



Scheme 1 Reaction conditions: (i) **5**, **9**, **13** (2.5 mmol); terminal alkyne (3–9 mmol), bis(PPh_3)PdCl₂ (0.375 mmol), Cu(I)I (0.357 mmol), DIPA (25 mL), 80 °C, 24 h; (ii) **6**, **10**, **14** (0.3–2 mmol), 10% Pd/C (10% wt eq), hexane or MeOH (10–100 mL), H_2 (3–15 bar), 20 °C, 16–72 h.; (iii) **7**, **11**, **15** (0.17–0.78 mmol), Rh(CAAC)-COD **17** (1.6 mol%), silica (0.2–1.6 g)/4 Å mol sieves (0.2–3.2 g), hexane (2–40 mL), H_2 (50–70 bar), 25–50 °C, 1–10 d.

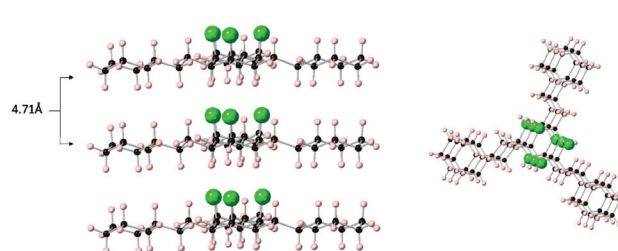


Fig. 3 Structure of **16e** showing perpendicular ring stacks in three isolated molecules.



highlights the Janus face character of this cyclohexane, with a highly negative (red) electrostatic potential associated with the triaxial fluorine face and a highly positive (blue) electrostatic potential associated with the triaxial hydrogens. On the other hand, the polarization diminishes considerably upon ring inversion, and the Janus face characteristic is lost for the triaxial alkyl groups in compound **4**. It is notable that the stacking of the cyclohexane rings in the tri-substituted derivatives further increases the attractive intermolecular interaction between positive and negative ring faces, as evidenced by the surface electrostatic potential maps for the dimer and trimer as illustrated in Fig. 4a, and by the interactions obtained through QTAIM and NCI calculations between axial fluorines and axial hydrogens (Fig. 4b and c, respectively).¹⁰ The strong attractive F–H interactions significantly stabilize these arrangements, with calculated complexation energies for the dimer and trimer of $-8.04 \text{ kcal mol}^{-1}$ and $-17.40 \text{ kcal mol}^{-1}$ respectively, the latter value essentially being the sum of two such intermolecular interactions. Therefore, it can be anticipated that it is the array of F···H contacts which are responsible for stabilizing the intermolecular cyclohexane interactions, leading to stabilization of the crystalline supramolecular assembly of the trialkyl-substituted cyclohexanes.

Only in the trisubstituted structures **16** are the ring stacks completely insulated from each other by the alkyl substituents. In the mono- and di-substituted systems *e.g.* **8** and **12c** there is lateral contact between fluorocyclohexane ring stacks (see ESI†)

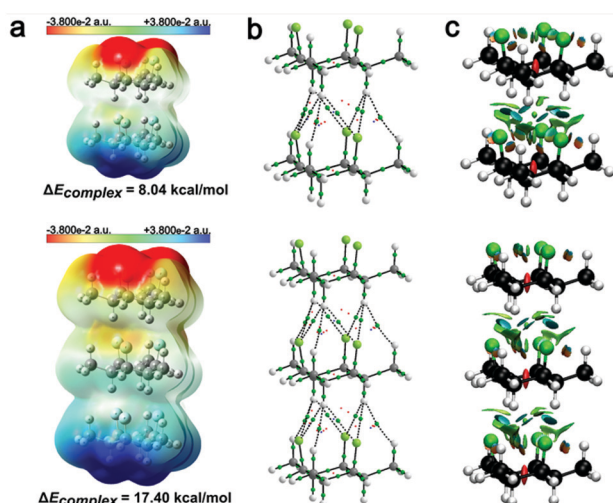


Fig. 4 (a) Surface electrostatic potential maps for dimeric and trimeric arrangements of the polar conformer of **4** obtained at the PBE0/def2-TZVP theory level. Both dimer and trimer are characterized by the electrostatic attraction between the hydrogen and fluorine faces. (b) QTAIM molecular graphics obtained from the PBE0/def2-TZVP electron density, with bond critical points (BCPs) represented by green spheres and ring critical points (RCPs) and cage critical points (CCPs) represented by small red and blue spheres, respectively. (c) NCI iso-surfaces obtained from PBE0/def2-TZVP electron density using reduced density gradient (RDG) = 0.5 and blue-green-red colour scale ranging from $-0.015 < \text{sign}(\lambda_2)\rho(r) < 0.015 \text{ a.u.}$ Complexation energies were calculated at B3LYP-D3/def2-TZVP optimised geometries using the HFLD method and with the aug-cc-pVTZ basis set.¹⁰

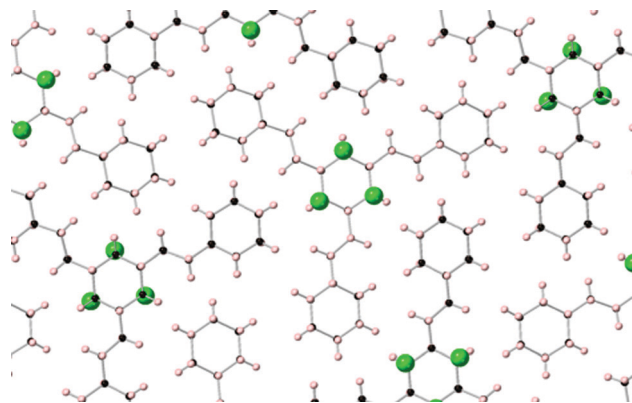


Fig. 5 The solid-state packing arrangements in the structure of **16e** showing that the all-syn fluorocyclohexane stacks are isolated and insulated laterally from each other by the hydrocarbon side chains. This is not the case for the mono- and di-substituted alkyl systems *e.g.* **8** and **12c** (see ESI†).

whereas there is a complete insulation of ring stacks in the solid-state structure of the trisubstituted compounds as illustrated for **16e** in Fig. 5. This suggests a characteristic of the trisubstituted systems in the solid-state.

Differential scanning calorimetry (DSC) and polarising optical microscopy (POM) analyses were carried out to assess if these materials were predisposed to polymorphism and/or liquid crystalline phases.¹¹ The analyses for compounds **16a–f** is presented in the ESI† and illustrated here for compound **16d** in Fig. 6. DSC analysis indicated that for some of the compounds only a single phase transition (melting point) was apparent, however for others, such as **16d**, there is clear polymorphic behaviour with a distinct transition at 97°C prior to melting at 141°C . The POM image of this polymorphic phase for **16d** has a clearly contrasted and highly orientated fibrous aspect typical of an ordered supramolecular structure, and this is found in several of the other systems too (see ESI† for **16a** & **16e**) although characteristics vary with different alkyl functionality.

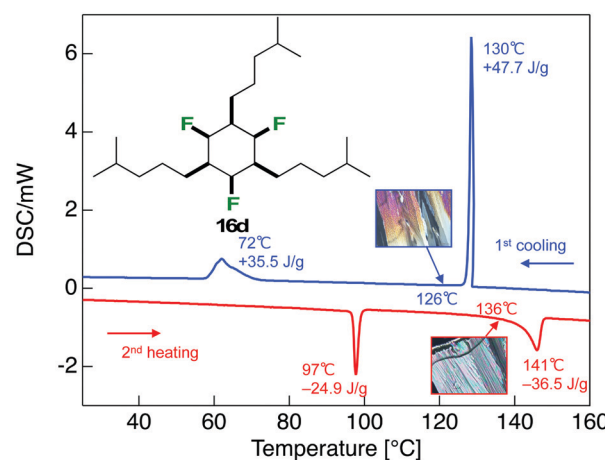


Fig. 6 DSC trace of **16d** illustrating polymorphic phases ($\text{mp} = 141^\circ\text{C}$) during the 1st cooling and 2nd heating cycle.



In conclusion we have presented a synthesis approach to selectively alkylated all-*syn* alkylated cyclohexanes that also contain triaxial C–F bonds, and we profile the alternating 2,4,6-trialkyl motifs in particular. The parallel orientation of the C–F bonds imparts a high polarity to these ring systems, and in selected cases the alkyl chains completely insulate the Janus ring stacks from each other, an arrangement which is not observed for the mono- and di-alkylated systems. The predisposition of the polar Janus rings to assemble in stacks due to electrostatic attraction between the alternating faces of the rings holds promise for ordering supramolecular assemblies with polar properties and offers an approach to designing next generation soft materials such as polar liquid crystals.

We thank the EPSRC for a studentship (TJP) through the CRITICAL Doctoral Training Centre. FAPESP is also gratefully acknowledged for a studentship (BAP, #2021/09716-5) and a Young Researcher Award (RAC, #2018/03910-1). CENAPAD-SP, CESUP and SDumont are also acknowledged for the computational resources used in theory calculations.

Conflicts of interest

There are no conflicts to declare.

References

- (a) C. Yu, A. Kütt, G.-V. Röschenthaler, T. Lebl, D. B. Cordes, A. M. Z. Slawin, M. Bühl and D. O'Hagan, *Angew. Chem., Int. Ed.*, 2020, **59**, 19905–19909; (b) D. O'Hagan, *Chem. – Eur. J.*, 2020, **26**, 7981–7997; (c) T. Bykova, N. Al-Maharik, A. M. Z. Slawin, M. Bühl, T. Lebl and D. O'Hagan, *Chem. – Eur. J.*, 2018, **24**, 13290–13296; (d) T. Bykova, N. Al-Maharik, A. M. Z. Slawin and D. O'Hagan, *Beilstein J. Org. Chem.*, 2017, **13**, 728–733; (e) M. Salah Ayoub, D. B. Cordes, A. M. Z. Slawin and D. O'Hagan, *Beilstein J. Org. Chem.*, 2015, **11**, 2671–2676.
- N. S. Keddie, A. M. Z. Slawin, T. Lebl, D. Philp and D. O'Hagan, *Nat. Chem.*, 2015, **7**, 483–488.
- (a) R. A. Cormanich, N. Keddie, R. Rittner, D. O'Hagan and M. Bühl, *Phys. Chem. Chem. Phys.*, 2015, **44**, 29475–29478; (b) B. E. Ziegler, M. Lecours, R. A. Marta, J. Featherstone, E. Fillion, W. S. Hopkins, V. Steinmetz, N. S. Keddie, D. O'Hagan and T. B. McMahon, *J. Am. Chem. Soc.*, 2016, **138**, 7460–7463; (c) M. J. Lecours, R. A. Marta, V. Steinmetz, N. Keddie, E. Fillion, D. O'Hagan, T. B. McMahon and W. S. Hopkins, *J. Phys. Chem. Lett.*, 2017, **8**, 109–113.
- (a) O. Shyshov, S. V. Haridas, L. Pesce, H. Y. Qi, A. Gardin, D. Bochicchio, U. Kaiser, G. M. Pavan and M. von Delius, *Nat. Commun.*, 2021, **12**, 3134; (b) A. Theodoridis, G. Papamokos, M. P. Wiesenfeldt, M. Wollenburg, K. Mullen, F. Glorius and G. Floudas, *J. Phys. Chem. B*, 2021, **125**, 3700–3709; (c) R. Mondal, M. Agbaria and Z. Nairoukh, *Chem. – Eur. J.*, 2021, **27**, 7193–7213.
- N. Santschi and R. Gilmour, *Nat. Chem.*, 2015, **7**, 467–468.
- (a) J. L. Clark, A. Taylor, A. Geddis, R. M. Neyyappadath, B. A. Piscelli, C. Yu, D. B. Cordes, A. M. Z. Slawin, R. A. Cormanich, S. Guldin and D. O'Hagan, *Chem. Sci.*, 2021, **12**, 9712–9719; (b) J. L. Clark, R. M. Neyyappadath, C. Yu, A. M. Z. Slawin, D. B. Cordes and D. O'Hagan, *Chem. – Eur. J.*, 2021, **27**, 16000–16005.
- H. Tsuji, G. Cantagrel, Y. Ueda, T. Chen, L. J. Wan and E. Nakamura, *Chem. – Asian J.*, 2013, **8**, 2377–2382.
- (a) T. Charvillat, P. Bernardelli, M. Daumas, X. Pannecoucke, V. Ferey and T. Besset, *Chem. Soc. Rev.*, 2021, **50**, 8178–8192; (b) Z. Nairoukh, M. Wollenburg, C. Schlepphorst, K. Bergander and F. Glorius, *Nat. Chem.*, 2019, **11**, 264–270; (c) M. P. Wiesenfeldt, Z. Nairoukh, W. Li and F. Glorius, *Science*, 2017, **357**, 908–912.
- (a) X. Zhang, L. Ling, M. Luo and X. Zeng, *Angew. Chem., Int. Ed.*, 2019, **58**, 16785–16789; (b) Y. Wei, B. Rao, X. Cong and X. Zeng, *J. Am. Chem. Soc.*, 2015, **137**, 9250–9253.
- (a) R. F. W. Bader, *Atoms in Molecules: A Quantum Theory*, Clarendon, Oxford, 1990; (b) J. Contreras-García, E. R. Johnson, S. Keinan, R. Chaudret, J. Piquemal, D. N. Beratan and W. Yang, *J. Chem. Theory Comput.*, 2011, **7**(3), 625–632; (c) A. Altun, F. Neese and G. Bistoni, *J. Chem. Theory Comput.*, 2019, **15**(11), 5894–5907.
- S. Yamada, M. Morita, Y. Wang, Q. Zhang, D. O'Hagan, T. Agou, H. Fukumoto, T. Kubota, M. Hara and T. Konno, *Crystals*, 2021, **11**, 450.